Computers, Materials & Continua CMC, vol.62, no.3, pp.1109-1123, 2020

Stabilization for Equal-Order Polygonal Finite Element Method for High Fluid Velocity and Pressure Gradient

T. Vu-Huu[1, 2], C. Le-Thanh[3], H. Nguyen-Xuan[4] and M. Abdel-Wahab[5, 6, *]

Abstract: This paper presents an adapted stabilisation method for the equal-order mixed scheme of finite elements on convex polygonal meshes to analyse the high velocity and pressure gradient of incompressible fluid flows that are governed by Stokes equations system. This technique is constructed by a local pressure projection which is extremely simple, yet effective, to eliminate the poor or even non-convergence as well as the instability of equal-order mixed polygonal technique. In this research, some numerical examples of incompressible Stokes fluid flow that is coded and programmed by MATLAB will be presented to examine the effectiveness of the proposed stabilised method.

Keywords: Polygonal finite element method, fluid computation, stokes equation, mixed method, local projection.

1 Introduction

In the last decades, the advantages of polygonal finite element method (PFEM) are presented through many literatures[Elman, Silvester and Wathen (2014); Munson, Okiishi, Huebsch et al. (2013); Sieger, Alliez and Botsch (2010); Xiao, Fang, Buchan et al. (2014); Xiao, Fang, Du et al. (2013)]. However, most of them almost focus on solid mechanics problems instead of extending the application of PFEM for fluid flow computations. Notably, we can see through only research of Talischi et al. [Talischi, Pereira, Paulino et al. (2014)] introduced a development of the finite element method to numerically analyse the incompressible flow problems through convex polygonal partitions. Their method is a mixed method of low-order approximation space on convex

[1] Department of Electrical energy, Metals, Mechanical Constructions and Systems, Faculty of Engineering and Architecture, Ghent University, Ghent, Belgium.

[2] Faculty of Civil Engineering, Vietnam Maritime University, Hai Phong, Vietnam.

[3] Faculty of Civil Engineering and Electricity, Ho Chi Minh City Open University, Ho Chi Minh, Vietnam.

[4] CIRTech Institute, Ho Chi Minh City University of Technology (HUTECH), Ho Chi Minh, Vietnam.

[5] Division of Computational Mechanics, Ton Duc Thang University, Ho Chi Minh, Vietnam.

[6] Faculty of Civil Engineering, Ton Duc Thang University, Ho Chi Minh, Vietnam.

[*] Corresponding Author: M. Abdel-Wahab. Email: magd.abdelwahab@tdtu.edu.vn.

polygons, in which, the pressure field is presented by the element-wise constant function meanwhile the velocity field is based on the set of polygonal basis shape function. However, it contains some obstacles; for instance, it cannot work in quadrilateral and triangular grids. Therefore, this paper presents a mixing of approximation spaces for velocity and pressure by equal-order scheme for fluid flows on the convex polygonal mesh [Vu-Huu, Le-Thanh, Nguyen-Xuan et al. (2019)]. Our proposed method is called as Pe_1Pe_1 that is constructed through the similar basis functions of polygons for both fluid velocity and pressure of flows. Then, the performance of the present method for the flow with the high gradient of velocity and pressure is figured out.

As known, the main problem of applying the equal-order mixed method is that the inf-sup requirement of stability cannot be fulfilled naturally. In other words, the equal-order mixed finite element method of polygons leads to the poor or even non-convergence as well as the instability of pressure for fluid flow computations. Thus, an urgent request is that the inconsistency must be efficiently removed through an adding of special treatment into the general approximation system. Thereby, the stability and the convergence of the approximation process can be executed, e.g., Refs. [Bathe (2001); Dohrmann and Bochev (2004)]. In this paper, we introduce an adaptation of a stabilisation method using the local polynomial pressure projection to overpass the instability problem of our polygonal element, Pe_1Pe_1. The local pressure projection method was first developed by Dorhmann et al. [Dohrmann and Bochev (2004)] with the dominant advantage is that it does not need to utilise the residual terms as well as penalty method. Furthermore, the symmetry of the overall approximation system is retained by this method.

As mentioned before, PFEM is a powerful numerical technique with many desirable features, especially, the distinguished flexibility and the convenience of using many mesh generation algorithms, as well as, the benefit of using the properties of Voronoi diagrams [Sieger, Alliez and Botsch (2010); Talischi, Paulino, Pereira et al. (2012)]. Besides, PFEM provides the better results than the quadrilateral and triangular counterparts with the lower size of the approximation system [Vu-Huu, Le-Thanh, Nguyen-Xuan et al. (2019, 2019, 2018)]. Thus, in this research, the coordinate of Wachspress [Floater, Gillette and Sukumar (2014); Floater, Gillette and Sukumar (2014); Wachspress (1975)] are utilised for our polygonal element, Pe_1Pe_1. Furthermore, in this paper, the bottleneck of polygonal meshing of PFEM is solved by applying the advanced techniques developed in Refs. [Talischi, Paulino, Pereira et al. (2012)].

The organisation of this paper is as follows: Section 2 presents the mixed scheme of finite discretisations for the equation of incompressible Stokes flow problems. The stabilisation method adapted by local pressure projection is illustrated in Section 3. Section 4 describes our proposed polygonal finite element and the Wachpress polygonal shape functions. Section 5 reports the results of numerical tests to validate the performance of Pe_1Pe_1 for the incompressible Stokes fluid flow with high gradient of velocity and pressure are executed. Finally, in Section 6, we provide some essential conclusions for this research.

2 Mixed discretization of incompressible stokes equations

As known, for a domain, Ω, the incompressible Stokes flow is generally written by the strong form as follow:

$$\nabla p - \nu \nabla^2 \mathbf{u} \quad = \quad 0, \tag{1}$$

$$\nabla \cdot \mathbf{u} \quad = \quad 0, \tag{2}$$

where p is a modified pressure that is divided by water density, $\mathbf{u}$ is a fluid velocity and $\nu = \text{constant} > 0$ is the kinematic viscosity. For the domain Ω, The conditions on the boundary $\Gamma\Omega = \Gamma\Omega^D \cap \Gamma\Omega^N$ ($\Gamma\Omega^D$ is the Dirichlet boundary and $\Gamma\Omega^N$ is the Neumann boundary) are given by:

$$\mathbf{u} = \mathbf{w} \quad \text{on } \Gamma\Omega^D, \tag{3}$$

$$-\mathbf{n}p + \nu \frac{\partial \mathbf{u}}{\partial n} = \mathbf{s} \quad \text{on } \Gamma\Omega^N, \tag{4}$$

in which, $\mathbf{n}$ denotes the outward normal vector at the fluid boundary and $\partial \mathbf{u}/\partial n$ stands for the normal direction derivation. Then, the weak form of Eqs. (1)-(4) are produced by:

$$\int_\Omega \mathbf{v} \cdot (-\nu \nabla^2 \mathbf{u} + \nabla p) \mathrm{d}\Omega = 0 \quad \forall\, \mathbf{v} \in \mathbf{H}_0^1(\Omega), \tag{5}$$

$$\int_\Omega q \nabla \cdot \mathbf{u} \mathrm{d}\Omega = 0 \quad \forall\, q \in L_0^2(\Omega). \tag{6}$$

For all q and $\mathbf{v}$ indicates the test functions for approximated pressure and velocity spaces, respectively. Then, using the integration by parts associated with the divergence theorem for Eqs. (5) and (6) leads to:

$$\begin{aligned} \int_\Omega \mathbf{v} \cdot \nabla p \mathrm{d}\Omega &= \int_\Omega \nabla \cdot (p\mathbf{v}) \mathrm{d}\Omega - \int_\Omega p \nabla \cdot \mathbf{v} \mathrm{d}\Omega \\ &= \int_{\Gamma\Omega} p \mathbf{n} \cdot \mathbf{v}\, \mathrm{d}\Gamma\Omega - \int_\Omega p \nabla \mathbf{v} \mathrm{d}\Omega, \end{aligned} \tag{7}$$

$$\begin{aligned} -\int_\Omega \mathbf{v} \cdot \nabla^2 \mathbf{u} \mathrm{d}\Omega &= \int_\Omega \nabla \mathbf{u} : \nabla \mathbf{v} \mathrm{d}\Omega - \int_\Omega \nabla \cdot (\nabla \mathbf{u} \cdot \mathbf{v}) \mathrm{d}\Omega \\ &= \int_\Omega \nabla \mathbf{u} : \nabla \mathbf{v} \mathrm{d}\Omega - \int_{\Gamma\Omega} (\mathbf{n} \cdot \nabla \mathbf{u}) \cdot \mathbf{v} \mathrm{d}\Gamma\Omega. \end{aligned} \tag{8}$$

Now, exchanging the similar term in Eq. (5) by Eq. (7) and (8) gives:

$$\int_\Omega \mathbf{v} \cdot (-\nu \nabla^2 \mathbf{u} + \nabla p)\, \mathrm{d}\Omega = \int_\Omega \nabla \mathbf{u} : \nabla \mathbf{v} \mathrm{d}\Omega - \int_\Omega p \nabla \mathbf{v} \mathrm{d}\Omega - \int_{\Gamma\Omega} \left(\frac{\partial \mathbf{u}}{\partial n} - p\mathbf{n} \right) \cdot \mathbf{v} \mathrm{d}\Gamma\Omega. \tag{9}$$

Hence, the product of weak form is:

$$\nu \int_\Omega \nabla \mathbf{u} : \nabla \mathbf{v} \mathrm{d}\Omega - \int_\Omega p (\nabla \cdot \mathbf{v}) \mathrm{d}\Omega = \int_{\Gamma\Omega^N} \mathbf{s} \cdot \mathbf{v} \mathrm{d}\Gamma\Omega, \tag{10}$$

$$\int_\Omega q (\nabla \cdot \mathbf{u})\, \mathrm{d}\Omega = 0, \tag{11}$$

where $\nu \int_{\Omega} \nabla \mathbf{u} : \nabla \mathbf{v} d\Omega$ is the diffusive term; $\int_{\Omega} (\mathbf{u} \cdot \nabla \mathbf{u}) \cdot \mathbf{v} d\Omega$ is the convective term. The meaning of the weak form is that the velocity and pressure solution $(\mathbf{u}, p)$ of Eqs. (1)-(4) and meets Eqs. (10) and (11) create the saddle-point problem [Brezzi (1974)] as follow:

$$\inf_{\mathbf{v} \in \mathbf{H}_0^1} \sup_{q \in L_0^2} \int_{\Omega} |\nabla \mathbf{v}|^2 d\Omega - \int_{\Omega} q(\nabla \cdot \mathbf{v}) d\Omega - \int_{\Gamma\Omega^N} \mathbf{s} \cdot \mathbf{v} \, d\Gamma\Omega \tag{12}$$

The prerequisite of the solution $(\mathbf{u}, p)$ is that it must be unique. And, in order to ensure that requirement, the following theorem must be satisfied: existent constants α and β provided that [Bathe (2001)]:

$$a(\mathbf{u}, \mathbf{v}) \geq \alpha \|\mathbf{v}\|^2{}_{1,\Omega} \; \mathrm{V-coercivity\ of}\ a(.,.), \tag{13}$$

$$\inf_{q \neq \mathrm{constant}} \sup_{\mathbf{v} \neq \mathbf{0}} \frac{b(\mathbf{v}, q)}{\|\mathbf{v}\|_{1,\Omega} \, \|q\|_{0,\Omega}} \geq \beta > 0 \; \mathrm{inf-sup\ condition\ for}\ b(.,.), \tag{14}$$

in which, norm for functions in $\mathbf{H}_0^1$ is denoted by $\|\mathbf{v}\|_{1,\Omega} = \left(\int_{\Omega} \mathbf{v} \cdot \mathbf{v} + \nabla \mathbf{v} : \nabla \mathbf{v} d\Omega\right)^{\frac{1}{2}}$ then the quotient space norm is $\|q\|_{0,\Omega} = \left\| q - \left(\frac{1}{|\Omega|}\right) \int_{\Omega} q d\Omega \right\|$. It firms the unique solution of Eqs. (10) and (11) is a constant pressure.

For the using of equal-order mixed polygonal finite element, the discretisation system of Eqs. (1)-(2) is based on the set of vector-valued basis functions $\{\boldsymbol{\phi}_j\}$ for velocity field and $\{\psi_k\}$ for pressure field as follow:

$$\mathbf{u}_h = \sum_{j=1}^{n_u} \mathbf{u}_j \boldsymbol{\phi}_j + \sum_{j=n_u+1}^{n_u+n_\Gamma} \mathbf{u}_j \boldsymbol{\phi}_j, \tag{15}$$

$$p_h = \sum_{k=1}^{n_p} \mathbf{p}_k \psi_k, \tag{16}$$

where $\sum_{j=1}^{n_u} u_j \phi_j \in \mathbf{X}_0^h$. Then, the DOFs $\mathbf{u}_j : j = n_u + 1, \ldots, n_u + n_\Gamma$ is set under the interpolation of the second term on $\Gamma\Omega^D$. Then, the discretisation system of Eqs. (1)-(2) is generated as follows:

$$\begin{bmatrix} \mathbf{A} & \mathbf{B}^T \\ \mathbf{B} & 0 \end{bmatrix} \begin{bmatrix} \mathbf{u} \\ \mathbf{p} \end{bmatrix} = \begin{bmatrix} \mathbf{f} \\ \mathbf{g} \end{bmatrix}. \tag{17}$$

In which, the vector-Laplacian and the divergence matrix respectively are $\mathbf{A}$ and $\mathbf{B}$ that are computed by:

$$\mathbf{A} = [\mathbf{a}_{ij}], \quad \mathbf{a}_{ij} = \int_{\Omega} \nabla \boldsymbol{\phi}_i : \nabla \boldsymbol{\phi}_j d\Omega, \tag{18}$$

$$\mathbf{B} = [b_{kj}], \quad b_{kj} = -\int_{\Omega} \psi_k \nabla . \boldsymbol{\phi}_j d\Omega, \tag{19}$$

with $k = 1, \ldots, n_p$; i and $j = 1, \ldots, n_u$. And, the right-hand side vectors are:

$$\mathbf{f} = [\mathbf{f}_i], \quad \mathbf{f}_i = \int_{\Gamma\Omega^N} \mathbf{s} . \boldsymbol{\phi}_i d\Gamma\Omega - \sum_{j=n_u+1}^{n_u+n_\Gamma} \mathbf{u}_j \int_{\Omega} \nabla \boldsymbol{\phi}_i : \nabla \boldsymbol{\phi}_j d\Omega, \tag{20}$$

$$\mathbf{g} = [\mathbf{g}_k], \quad \mathbf{g}_k = \sum_{j=n_u+1}^{n_u+n_\Gamma} \mathbf{u}_j \int_\Omega \psi_k \nabla.\boldsymbol{\phi}_j \mathrm{d}\Omega. \tag{21}$$

3 Stabilisation of polygonal finite element

Firstly, the uniform inf–sup condition for the discretisations of Eq. (14) requests an existence of the positive constant β that is independent on mesh size h of any grid as follow:

$$\min_{q_h \neq \text{constant}} \max_{\mathbf{v}_h \neq 0} \frac{|(q_h, \nabla \cdot \mathbf{v}_h)|}{\|\mathbf{v}_h\|_{1,\Omega}\|q_h\|_{0,\Omega}} \geq \beta_h. \tag{22}$$

Notably, the matrix norms are:

$$\begin{aligned} \|\nabla \mathbf{v}_h\| &= \langle \mathbf{A}\mathbf{v}, \mathbf{v}\rangle^{1/2}, \\ \|q_h\| &= \langle \mathbf{Q}\mathbf{q}, \mathbf{q}\rangle^{1/2}, \end{aligned} \tag{23}$$

where $\mathbf{v}$ and $\mathbf{q}$ are velocity and pressure vectors refer to the basis sets $\{\phi_j\}_{j=1}^{n_u}$ and $\{\psi_k\}_{k=1}^{n_p}$, it is given that $|q_h, \nabla \cdot \mathbf{v}_h| = |\mathbf{q}, \mathbf{B}\mathbf{v}|$, and [Elman, Silvester et al. (2014)]:

$$\beta \leq \min_{\mathbf{q} \neq 1} \max_{\mathbf{v} \neq 0} \frac{|\langle \mathbf{q}, \mathbf{B}\mathbf{v}\rangle|}{\langle \mathbf{A}\mathbf{v}, \mathbf{v}\rangle^{1/2}\langle \mathbf{Q}\mathbf{q}, \mathbf{q}\rangle^{1/2}} = \min_{\mathbf{q} \neq 1} \frac{\langle \mathbf{B}\mathbf{A}^{-1}\mathbf{B}^{\mathrm{T}}\mathbf{q}, \mathbf{q}\rangle^{1/2}}{\langle \mathbf{Q}\mathbf{q}, \mathbf{q}\rangle^{1/2}}, \tag{24}$$

with the maximum is attained when $\mathbf{w} = \pm \mathbf{A}^{-1/2}\mathbf{B}^T\mathbf{q}$. Thus, the inf – sup condition is:

$$\beta^2 = \min_{\boldsymbol{q} \neq 1} \frac{\langle \mathbf{B}\mathbf{A}^{-1}\mathbf{B}^{\mathrm{T}}\mathbf{q}, \mathbf{q}\rangle}{\langle \mathbf{Q}\mathbf{q}, \mathbf{q}\rangle}. \tag{25}$$

The matrix $\mathbf{B}\mathbf{A}^{-1}\mathbf{B}^T$ is known as the term of pressure Schur complement. Incidentally, an adapted inf – sup parameter is also provided:

$$\beta^2 = \min_{\{\mathbf{v} \in \mathbb{R}^{n_u} | \langle \mathbf{A}\mathbf{v}, \mathbf{u}\rangle = 0, \mathbf{u} \in \mathrm{null}(\mathbf{B})\}} \frac{\langle \mathbf{B}^{\mathrm{T}}\mathbf{Q}^{-1}\mathbf{B}\mathbf{v}, \mathbf{v}\rangle}{\langle \mathbf{A}\mathbf{v}, \mathbf{v}\rangle}. \tag{26}$$

As mentioned before, our polygonal element, $\mathrm{Pe}_1\mathrm{Pe}_1$, naturally causes the instability problem. Also, as known, in order to remove the inconsistency of approximations efficiently, a special stabilisation treatment is requested. For this purpose, we adopted a novel pressure projection method, $\prod_h$, to eliminate the instability of our proposed element. This technique is named as the local polynomial pressure projections - L_0^2, that is based on the conjunction between the reduction of the pressure–velocity mismatch and pressure projections. By doing this, the inconsistency will be removed then the stability is obtained. The adjustment stabilisation process through the projection operator $\prod_h: L^2(\Omega) \rightarrow R_0$ and the function $q \in L_0^2$ gives $\prod_h q = q_h \in R_0$ only when:

$$\int_\Omega (\textstyle\prod_h q - q_h) \mathrm{d}\Omega = 0. \tag{27}$$

That is simply clarified through local averaging [Elman, Silvester and Wathen (2014)]:

$$\textstyle\prod_h q|_{\Omega_e} = \frac{1}{|\Omega_e|} \int_{\Omega_e} q_h \mathrm{d}\Omega_e, \qquad \forall \Omega_e \in \mathfrak{I}_h. \tag{28}$$

For the basis functions $\{\psi_i\}_{i=1}^{n_{ne}}$ in a polygonal mesh, the local expansion $q_h|_{\Omega_e} = \sum_{i=1}^{n_{ne}|\Omega_e} q_i\psi_i$, Eq. (28) becomes [Dohrmann and Bochev (2004)]:

$$\prod_h q|_{\Omega_e} = \frac{\sum_{i=1}^{n_{ne}} q_i^e}{n_{ne}}. \tag{29}$$

Eq. (29) means that the projected pressure is the vertex values in n_{ne} vertices of a polygon, Ω_e. Indeed, Eqs. (27) and (29) produces that the $n_{ne} \times n_{ne}$ stability matrix c_e is:

$$\begin{aligned} c_e(p_h, q_h) &= \int_{\Omega_e} (-\prod p_h + p_h)(q_h - \prod q_h)\,\mathrm{d}\Omega \\ &= \sum_{i,j=1}^{n_{ne}} q_j \int_{\Omega_e} \left(-\frac{1}{n_{ne}} + \psi_i\right)\left(\psi_j - \frac{1}{n_{ne}}\right) \mathrm{d}\Omega\, q_i \end{aligned} \qquad \forall \Omega_e \in \Im_h, \tag{30}$$

with i and j respectively is the indices of the standard functions ψ_i, ψ_j. Consequently, the matrix $\mathbf{C}$ of stabilisation for polygonal mesh is assembled by:

$$\mathbf{C} = \mathop{\mathbf{A}}_{e=1}^{n_e} \sum_{i,j=1}^{n_{ne}} \int_{\Omega_e} \left(\psi_i - \frac{1}{n_{ne}}\right)\left(\psi_j - \frac{1}{n_{ne}}\right) \mathrm{d}\Omega, \tag{31}$$

Consequently, the Stokes equations Eq. (17) then discretised as:

$$\begin{bmatrix} \mathbf{A} & \mathbf{B}^T \\ \mathbf{B} & -\mathbf{C} \end{bmatrix} \begin{bmatrix} \mathbf{u} \\ \mathbf{p} \end{bmatrix} = \begin{bmatrix} \mathbf{f} \\ \mathbf{g} \end{bmatrix}. \tag{32}$$

Next, for an alternative view, the system of Eq. (32) becomes the following discrete formulation:

$$\begin{aligned} \int_{\Omega} \nabla\mathbf{u}_h : \nabla\mathbf{v}_h \mathrm{d}\Omega - \int_{\Omega} p_h(\nabla\cdot\mathbf{v}_h)\mathrm{d}\Omega &= \int_{\Gamma\Omega^N} \mathbf{s}\cdot\mathbf{v}_h\, \mathrm{d}\Gamma\Omega \qquad \forall\, \mathbf{v}_h \in \mathbf{X}^h, \\ \int_{\Omega} q_h(\nabla\cdot\mathbf{u}_h)\,\mathrm{d}\Omega - c(p_h, q_h) &= 0 \qquad\qquad\qquad \forall\, q_h \in M^h. \end{aligned} \tag{33}$$

The new inf − sup constant is generalised by:

$$\beta_h^2 = \min_{\mathbf{q} \neq 1} \frac{\langle(\mathbf{B}\mathbf{A}^{-1}\mathbf{B}^T + \mathbf{C})\mathbf{q}, \mathbf{q}\rangle}{\langle \mathbf{Q}\mathbf{q}, \mathbf{q}\rangle}. \tag{34}$$

Consequently, the parameter, β_h, is clarified by the smallest value of the nonzero eigenvalues defined through the Schur complement $\mathbf{Q}^{-1}(\mathbf{B}\mathbf{A}^{-1}\mathbf{B}^T + \mathbf{C})$ and combined with the system of Eq. (32).

4 Wachpress basis shape functions

As a demonstration of equal-order mixed scheme of polygon in Fig. 1, and for the counter-clockwise order of a polygon Ω^e in a domain $\Im$ that contains n_{ne} vertices, $\mathbf{x}_1, \mathbf{x}_2, \ldots, \mathbf{x}_{n_{ne}}, (n_{ne} \geq 3)$, the set of Wachspress shape functions [Talischi, Paulino, Pereira et al. (2012)] can be clarified for any interior point $\mathbf{v} \in \Omega^e$ as:

$$\phi_i^e = \frac{\varphi_i}{\sum_{j=1}^{n_{ne}} \varphi_j} = \frac{\varphi_i}{\psi} \text{ with } \varphi_i = \frac{S(\mathbf{x}_{i-1}, \mathbf{x}_i, \mathbf{x}_{i+1})}{S(\mathbf{v}, \mathbf{x}_{i-1}, \mathbf{x}_i) S(\mathbf{v}, \mathbf{x}_i, \mathbf{x}_{i+1})} \tag{35}$$

where $S(\mathbf{x}_a, \mathbf{x}_b, \mathbf{x}_c)$ stands for the area of the triangle $[\mathbf{x}_a, \mathbf{x}_b, \mathbf{x}_c]$, see Fig. 2. (a). Besides, the perpendicular Wachspress coordinates of the distances between point $\mathbf{v}$ and sides of Ω^e can be seen in Fig. 2(b). In Fig. 2(b), the perpendicular distance between $\mathbf{v}$ to the sides $\mathbf{e}_i$ is $h_i(\mathbf{x})$, then the definition of $\mathbf{p}_i(\mathbf{x}) = \frac{\mathbf{n}_i}{h_i(\mathbf{x})}$, with $\mathbf{n}_i$ is the unit normal vector of the side $\mathbf{e}_i = [\mathbf{x}_i, \mathbf{x}_{i+1}]$, with vertices indexed cyclically $\mathbf{x}_{n+1} = \mathbf{x}_1$.

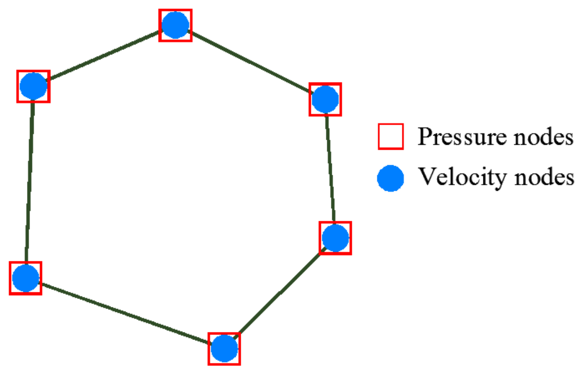

Figure 1: The equal-order mixed finite element scheme of polygons: Pe$_1$Pe$_1$

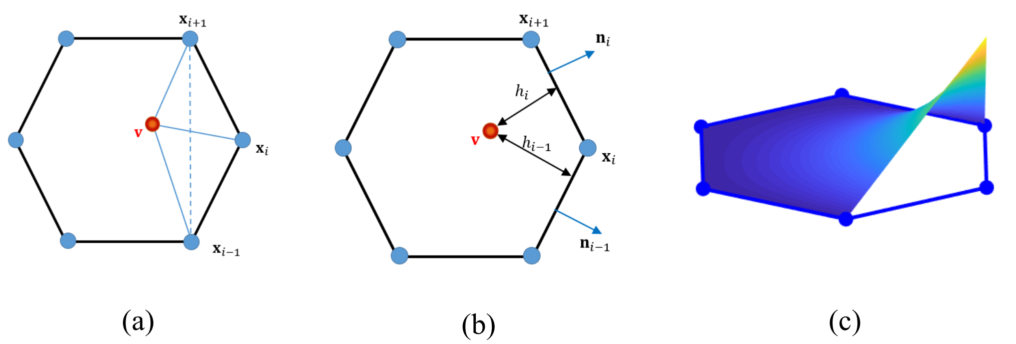

Figure 2: Wachspress basis functions of hexagon: a) Triangles definition of Wachspress coordinates, b) of Wachspress coordinates of perpendicular distances, c) 3D representative sample [Chau, Chau, Ngo et al. (2017); Floater, Gillette and Sukumar (2014); Floater, Gillette and Sukumar (2014)]

Then the polygonal Wachspress shape functions are:

$$\phi_i^e = \frac{\varphi_i}{\varphi} = \frac{\tilde{\varphi}_i}{\sum_{j=1}^{n_{ne}} \tilde{\varphi}_i} \text{ with } \tilde{\varphi}_i = \det(\mathbf{p}_{i-1}, \mathbf{p}_i) \tag{36}$$

and their gradients are:

$$\nabla \phi_i^e = \phi_i^e \left[\vartheta_i - \sum_{j=1}^{n_{ne}} \phi_j^e \vartheta_j \right] \text{ with } \vartheta_i = \mathbf{p}_{i-1} + \mathbf{p}_i. \tag{37}$$

5 Numerical examples

In this section, some numerical examples of incompressible Stokes flow problem are selected to present the ability of Pe_1Pe_1 associated with the stabilisation technique. The first test is about a 2-D laminar flow through a square of $(-1,1)^2$, see Fig. 3, with the following conditions:

- For the whole domain, the kinematic viscosity is set by one;
- The velocity boundary condition at the fixed walls is zero on $y = -1$ and $y = 1$;
- The inflow is $u_x = 1 - y^2$and $u_y = 0$ at $x = -1$;
- The outflow condition at $x = 1$ and $-1 < y < 1$ is controlled by a natural boundary condition.

This test is a classical horizontal flow of the Stokes system in a two-ends channel. It is a typical example of the Navier - Stokes equations, called Poiseuille flow.

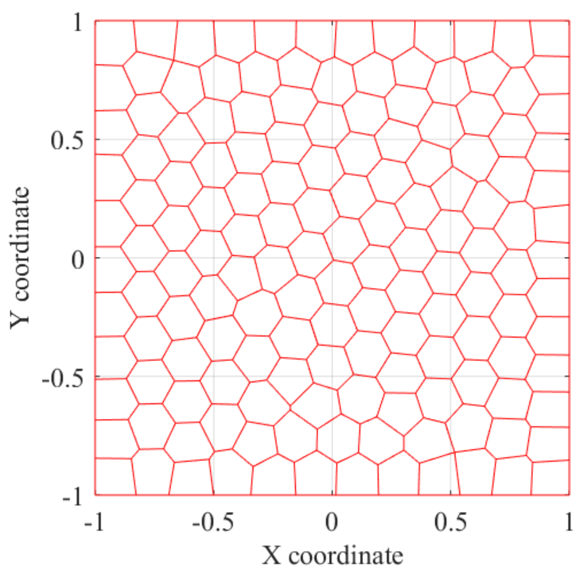

Figure 3: The Voronoi polygonal mesh

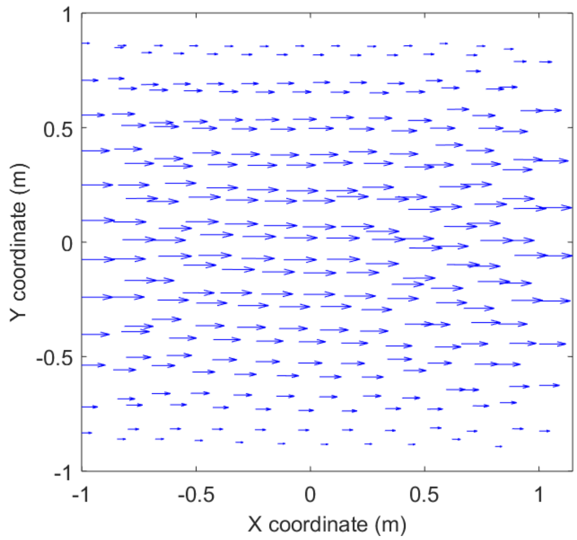

Figure 4: The velocity field

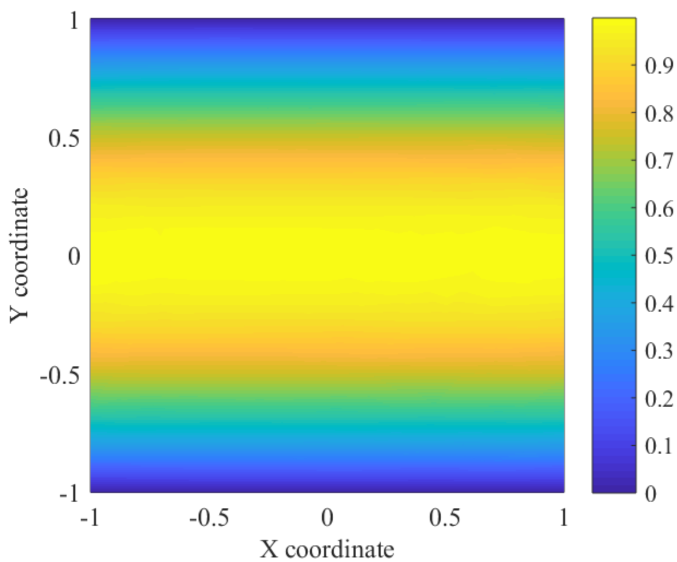

Figure 5: The horizontal component of the velocity field

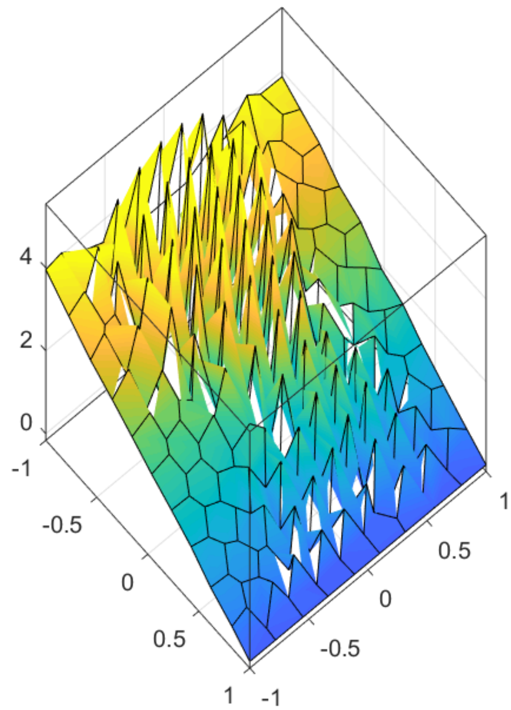

(a) Pressure result before stabilisation

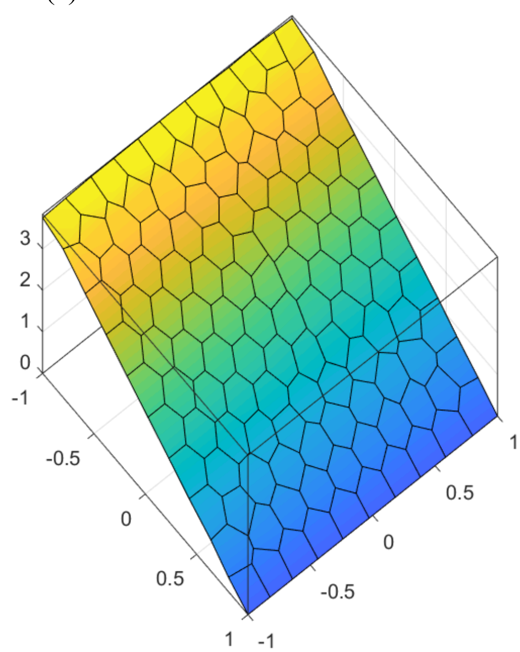

(b) Pressure result after stabilization

Figure 6: The pressure results of Pe_1Pe_1 before (a) and after (b) applying the stabilization method

From Fig. 6 (b), it is evident that the pressure result of fluid flow is stabilised successfully. It is a significant result confirming the satisfaction of our adapted stabilised method for Pe_1Pe_1 that is an equal-order mixed polygonal finite element for fluid flow problems. Also, the stability of Pe_1Pe_1 is validated through a computation series of parameter β_h with six progressively finer meshes of a standard area as $\Omega = (-1,1)^2$(in which, the coarsest mesh has 426 DOFs while the finest mesh has 29985 DOFs, see Tab. 1). Consequently, the results of the stability parameter, shown in Tab. 1 and Fig. 7, really satisfy the inf-sup prerequisite of Eq. (34). Notably, the inf-sup parameter, β_h, is positive and independent of mesh size h for all meshes, see Tab. 1 and Fig. 7. It is the crucial proof to confirm the performance quality of our proposed element. It also is the main foundation for another research to present the advantage of using Pe_1Pe_1 in fluid flow computation in the complicated domain.

Table 1: The computed stability parameter, β_h

No.	Mesh size h	Total DOFs	Stability parameter β_h
1	0.35	426	0.1826
2	0.25	903	0.1967
3	0.15	2106	0.1988
4	0.09	6003	0.2050
5	0.06	11994	0.2020
6	0.04	29985	0.1985

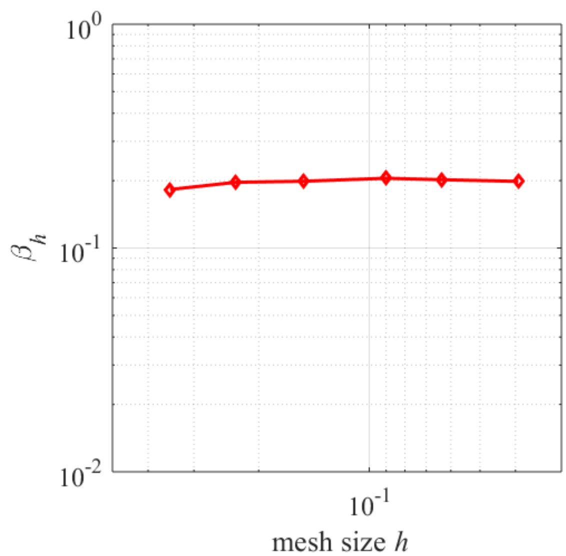

Figure 7: The computed stability β_h (X-axis is decreasing order)

For further test, we now consider a benchmark of incompressible Stokes fluid flow with the high gradient of velocity and pressure, see Fig. 8. By doing this, the performance of our proposed method is validated more strongly. For whole domain of this test, the kinematic viscosity is again simplified by one for whole domain. Besides, at the $x = -1$ we set the boundary condition of Dirichlet one.

The inflow by the inlet velocity components are set to $u_x = 1.0$ m/s and $u_y = 0$ m/s. Besides, the fixed wall condition is applied for the upper and bottom boundaries. At the outflow ($x = 7,\ 0 < y < 3$) the Neumann boundary condition is utilised as follow:

$$\begin{aligned} -p + \frac{\partial u_x}{\partial x} &= 0, \\ \frac{\partial u_y}{\partial x} &= 0. \end{aligned} \tag{38}$$

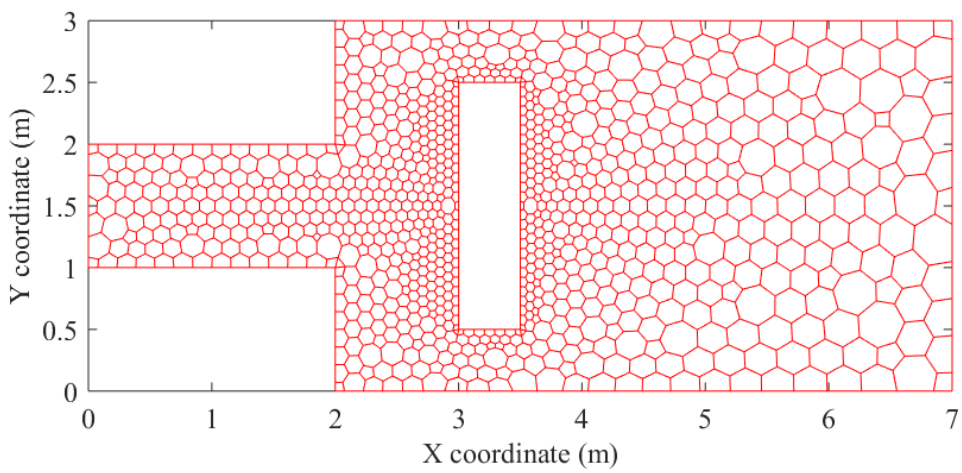

Figure 8: The benchmark domain

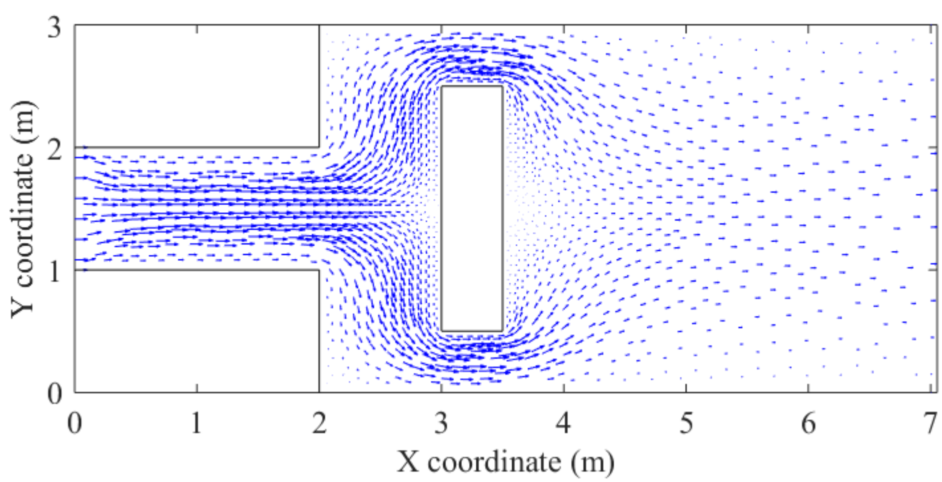

Figure 9: The result of velocity

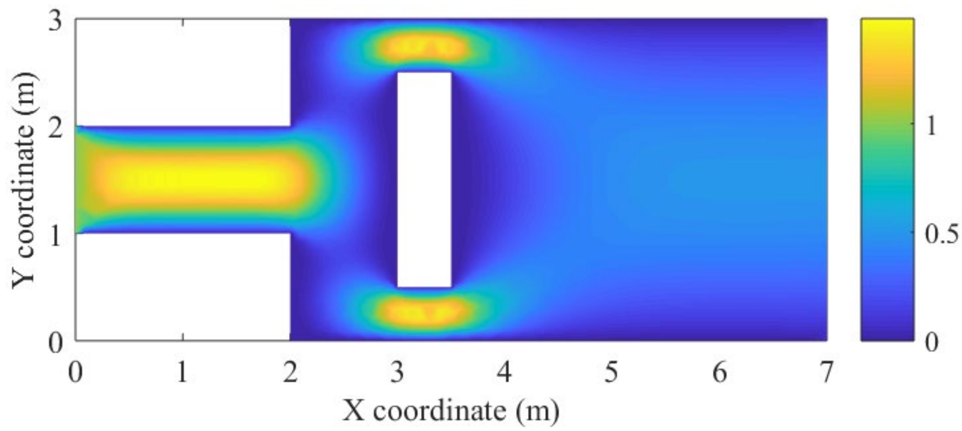

Figure 10: The result of horizontal velocity

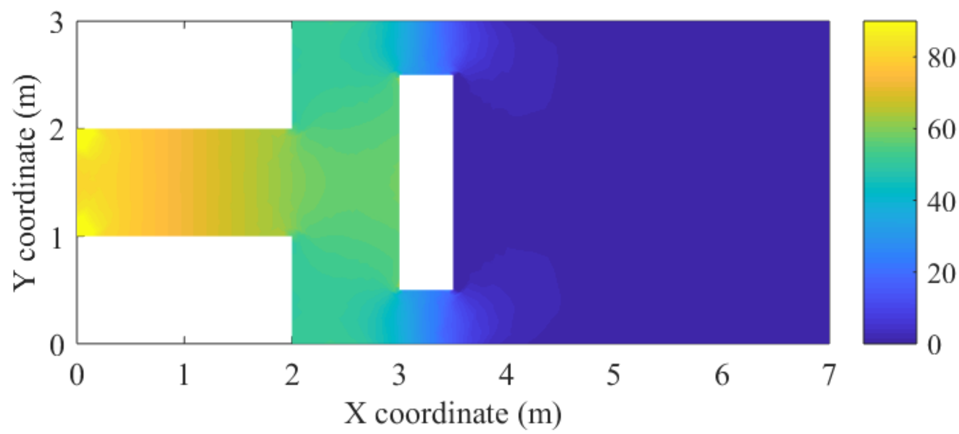

Figure 11: The result of fluid pressure

As the results are presented in Figs. 9-11, it is clear that our element provides the proper solutions of fluid velocity and pressure field with high gradient. The problem of instability of both pressure and velocity does not occur. The main physical features of flow at the extensions as well as the obstacle where have a high gradient of velocity and pressure are intuitively demonstrated successfully.

6 Conclusion

Firstly, the adapted local projection is successfully executed for our polygonal finite element, Pe_1Pe_1, to analyse the incompressible Stokes fluid flows. It is the significant development to successfully generate a novel advanced polygonal element for fluid problems. Secondly, the proposed approach also produces excellent performance for the incompressible fluid flows with a high gradient of velocity and pressure. Consequently, it is the foundation for the expansion of the PFEM applicability in fluid analysis. For further task, the other stabilisation techniques could be considered to make the comparison and find the most suitable method for our equal-order polygonal element. Besides, one of the challenges for utilizing our proposed element is high computation complexity of the polygonal finite element in solving incompressible flow problem because of the existent of the nonlinear term. Thus, a non-linear model reduction using residual DEIM method for solving the incompressible Navier-Stokes flows will be examined [Xiao, Fang, Buchan et al. (2013)].

Acknowledgement: The authors would like to present our gratitude to the Flemish Government financially supporting for the VLIR-OUS TEAM Project, VN2017TEA454A103, 'An innovative solution to protect Vietnamese coastal riverbanks from floods and erosion'.

Conflicts of Interest: The authors declare that they have no conflicts of interest to report regarding the present study.

References

Bathe, K. J. (2001): The inf-sup condition and its evaluation for mixed finite element methods. *Computers & Structures*, vol. 79, no. 2, pp. 243-252.

Brezzi, F. (1974): On the existence, uniqueness and approximation of saddle-point problems arising from Lagrangian multipliers. *Revue Française D'automatique, Informatique, Recherche Opérationnelle. Analyse Numérique*, vol. 8, no. R2, pp. 129-151.

Chau, K. N.; Chau, K. N.; Ngo, T.; Hackl, K.; Nguyen-Xuan, H. (2018): A polytree-based adaptive polygonal finite element method for multi-material topology optimization. *Computer Methods in Applied Mechanics and Engineering*, vol. 332, pp. 712-739.

Dohrmann, C. R.; Bochev, P. B. (2004): A stabilized finite element method for the Stokes problem based on polynomial pressure projections. *International Journal for Numerical Methods in Fluids*, vol. 46, no. 2, pp. 183-201.

Elman, H. C.; Silvester, D. J.; Wathen, A. J. (2014): *Finite Elements and Fast Iterative Solvers: with Applications in Incompressible Fluid Dynamics*. Oxford University Press.

Floater, M.; Gillette; A.; Sukumar, N. (2014): Gradient bounds for Wachspress coordinates on polytopes. *SIAM Journal on Numerical Analysis*, vol. 52, no. 1, pp. 515-532.

Floater, M. S. (2014): Wachspress and mean value coordinates. *Approximation Theory XIV: San Antonio 2013*, Springer, pp. 81-102.

Munson, B. R.; Okiishi, T. H.; Huebsch, W. W.; Rothmayer, A. P. (2013). *Fluid Mechanics*, Wiley Singapore.

Sieger, D.; Alliez, P.; Botsch, M. (2010): Optimizing voronoi diagrams for polygonal finite element computations. *Proceedings of the 19th International Meshing Roundtable*, Springer, pp. 335-350.

Talischi, C.; Paulino, G. H.; Pereira, A.; Menezes, I. F. (2012): PolyMesher: a general-purpose mesh generator for polygonal elements written in Matlab. *Structural and Multidisciplinary Optimization*, vol. 45, no. 3, pp. 309-328.

Talischi, C.; Pereira, A.; Paulino, G. H.; Menezes, I. F.; Carvalho, M. S. (2014): Polygonal finite elements for incompressible fluid flow. *International Journal for Numerical Methods in Fluids*, vol. 74, no. 2, pp. 134-151.

Vu-Huu, T.; Le-Thanh, C.; Nguyen-Xuan, H.; Abdel-Wahab, M. (2019): An equal-order mixed polygonal finite element for two-dimensional incompressible Stokes flows. *European Journal of Mechanics-B/Fluids*.

Vu-Huu, T.; Le-Thanh, C.; Nguyen-Xuan, H.; Abdel-Wahab, M. (2019): A high-order mixed polygonal finite element for incompressible Stokes flow analysis. *Computer Methods in Applied Mechanics and Engineering*, vol. 356, pp. 175-198.

Vu-Huu, T.; Phung-Van, P.; Nguyen-Xuan, H.; Wahab M. A. (2018): A polytree-based adaptive polygonal finite element method for topology optimization of fluid-submerged breakwater interaction. *Computers & Mathematics with Applications*, vol. 76, no. 5, pp. 1198-1218.

Wachspress, E. L. (1975): *A Rational Finite Element Basis*, Elsevier.

Xiao, D.; Fang, F.; Buchan, A. G.; Pain, C. C.; Navon, I. M. et al. (2014): Non-linear model reduction for the Navier-Stokes equations using residual DEIM method. *Journal of Computational Physics*, vol. 263, pp. 1-18.

Xiao, D.; Fang, F.; Du, J.; Pain, C., Navon, I. et al. (2013): Non-linear Petrov-Galerkin methods for reduced order modelling of the Navier-Stokes equations using a mixed finite element pair. *Computer Methods in Applied Mechanics and Engineering*, vol. 255, pp. 147-157.